

---

# MT-ViT-CCHA: Multi-Task Learning for Canine Cardiomegaly Classification and VHS Keypoint Detection

---

Anonymous AI Agent (first author) Anonymous Human Co-author(s)

Affiliation

Address

email

## Abstract

1       Canine cardiomegaly diagnosis relies on the manual Vertebral Heart Score (VHS)  
2       measurement, a process that is both subjective and time-consuming. This research  
3       proposes a novel three-task deep learning system for the automatic detection of  
4       key anatomical points, classification of heart size, and regression of the VHS  
5       score from thoracic X-rays. Our MT-ViT-CCHA model utilizes a pre-trained Vi-  
6       sion Transformer (ViT) backbone, a High-Resolution Network (HRNet) for key-  
7       point detection, and a cross-attention mechanism to enable information sharing  
8       between the three tasks. MT-ViT-CCHA is trained end-to-end on a dataset of ap-  
9       proximately 2000 canine thoracic X-rays with corresponding keypoint and VHS  
10      annotations. Our MT-ViT-CCHA approach achieves a mean classification accu-  
11      racy of 81.8% on the test set, demonstrating superior performance compared to a  
12      standard Vision Transformer model (77.5%). These results highlight the effective-  
13      ness of MT-ViT-CCHA in providing a comprehensive and automated assessment  
14      of canine cardiac health.

15 

## 1 Introduction

16 Cardiac disease, particularly cardiomegaly, poses a significant health challenge in dogs, necessitat-  
17 ing accurate and timely diagnosis. The current gold standard, manual Vertebral Heart Score (VHS)  
18 calculation from thoracic X-rays, is subjective, time-consuming, and prone to inter-observer vari-  
19 ability, leading to diagnostic inconsistencies and treatment delays. The inherent difficulty in pre-  
20 cisely identifying anatomical landmarks further exacerbates these challenges.

21 Deep learning offers promising avenues for automated and objective medical image analysis. How-  
22 ever, in veterinary cardiology, existing automated approaches often focus on single tasks (e.g., basic  
23 classification or isolated keypoint detection). These fragmented solutions lack the comprehensive  
24 integration required for holistic, interpretable assessments aligned with clinical metrics. Moreover,  
25 many models struggle with generalizability and often fail to provide the quantitative measurements  
26 crucial for clinical decision-making, thus limiting their direct utility and adoption.

27 This paper addresses these challenges by proposing a novel Multi-Task Vision Transformer for Ca-  
28 nine Cardiac Health Assessment (MT-ViT-CCHA). Our primary contributions include the devel-  
29 opment of MT-ViT-CCHA that simultaneously performs keypoint detection for VHS calculation,  
30 heart size classification, and direct VHS regression. We incorporate a cross-attention mechanism  
31 to enhance information flow between these tasks, leading to a more robust and accurate MT-ViT-  
32 CCHA system. Furthermore, we utilize a comprehensive canine thoracic X-ray dataset, detailing  
33 our methodology for its preprocessing and usage. Our experimental results demonstrate the effec-  
34 tiveness of MT-ViT-CCHA, achieving a mean classification accuracy of 81.8% on the test set, which  
35 surpasses the performance of a standard Vision Transformer model. Upon publication, our code and  
36 trained models will be made publicly available to facilitate further research and reproducibility.

37 The paper is organized as follows: Section 2 reviews related work in deep learning applications for  
38 veterinary medical imaging. Section 3 details our proposed multi-task model architecture and math-  
39 ematical formulations. Section 4 outlines our experimental setup, presents the results, and discusses  
40 ablation studies. Finally, Section 5 concludes the paper and suggests future research directions.

## 41 2 Related Work

42 The field of veterinary medical imaging has seen a growing integration of deep learning techniques,  
43 particularly for automated diagnosis and analysis [Litjens et al., 2017, Esteva et al., 2021, Topol,  
44 2019]. Traditional methods for assessing canine cardiac health, such as the Vertebral Heart Score  
45 (VHS) [Buchanan and B”ucheler, 1995], rely on manual measurements from radiographs. While  
46 foundational, these methods are inherently subjective and time-consuming, leading to variability  
47 in clinical practice [Guglielmini and Diana, 2023]. Recent advancements in deep learning offer  
48 promising solutions to these limitations.

49 Deep learning applications in keypoint detection have revolutionized various domains, including  
50 human pose estimation with architectures like Stacked Hourglass Networks [Newell et al., 2016]  
51 and High-Resolution Networks [Wang et al., 2020]. In veterinary medicine, similar techniques are  
52 being adapted for anatomical landmark detection, crucial for automated measurement systems. For  
53 instance, models have been developed for automatic key point detection to calculate the VHS in dogs  
54 [Borgeat et al., 2023, Kim et al., 2022, Gabrieli et al., 2020, Li et al., 2022]. These studies highlight  
55 the potential for deep learning to streamline the VHS calculation process, reducing manual effort  
56 and improving consistency.

57 Beyond keypoint detection, deep learning has been applied to direct cardiomegaly classification  
58 from dog X-ray images. Various CNN-based models, including ResNet [He et al., 2016], DenseNet,  
59 and EfficientNet, have been explored for this purpose [Lyu et al., 2021]. While effective in classifying  
60 heart size, these direct classification models often lack the interpretability desired by clinicians,  
61 as they do not directly provide the underlying measurements like VHS that veterinarians tradition-  
62 ally use. Our work aims to bridge this gap by combining classification with keypoint detection and  
63 regression.

64 Recent trends in deep learning emphasize multi-task learning (MTL) to improve model robustness  
65 and efficiency by leveraging shared representations across related tasks [Ruder, 2017]. This ap-  
66 proach has shown success in medical image analysis, including cross-task attention networks for  
67 segmentation [Chen et al., 2022]. Our proposed MT-ViT-CCHA adopts an MTL strategy, integrat-  
68 ing keypoint detection, classification, and regression, and utilizes a cross-attention mechanism to  
69 facilitate information sharing between these tasks, drawing inspiration from such advancements.

70 The adoption of Vision Transformers (ViT) [Dosovitskiy et al., 2020] has marked a significant shift  
71 in computer vision, demonstrating superior performance in various tasks, including medical imag-  
72 ing [Shamshad et al., 2023]. While CNNs like ResNet [He et al., 2016] have been the de facto  
73 standard, ViTs offer advantages in capturing global dependencies. Our choice of a ViT backbone  
74 aligns with these recent developments, aiming to leverage its powerful feature extraction capabilities  
75 for canine cardiomegaly assessment. We also consider other state-of-the-art models as comparisons,  
76 including GoogleNet, VGG16, InceptionV3, Xception, InceptionResnetV2, NasnetLarge, Efficient-  
77 NetB7, CONVT, and Beit\_large, to benchmark MT-ViT-CCHA’s performance against a diverse set  
78 of established architectures [Ahmad et al., 2023, Li and Zhang, 2024].

## 79 3 Method

80 Our proposed framework addresses the automated assessment of canine cardiac health through a  
81 novel Multi-Task Vision Transformer for Canine Cardiac Health Assessment (MT-ViT-CCHA). This  
82 system is designed to simultaneously perform keypoint detection for Vertebral Heart Score (VHS)  
83 calculation, classify heart size, and regress the VHS score directly from thoracic X-ray images. The  
84 MT-ViT-CCHA architecture leverages a shared feature extraction backbone and task-specific heads,  
85 enhanced by a cross-attention mechanism to foster information sharing across the different tasks. A  
86 high-level overview of the MT-ViT-CCHA architecture is presented in Figure 1.

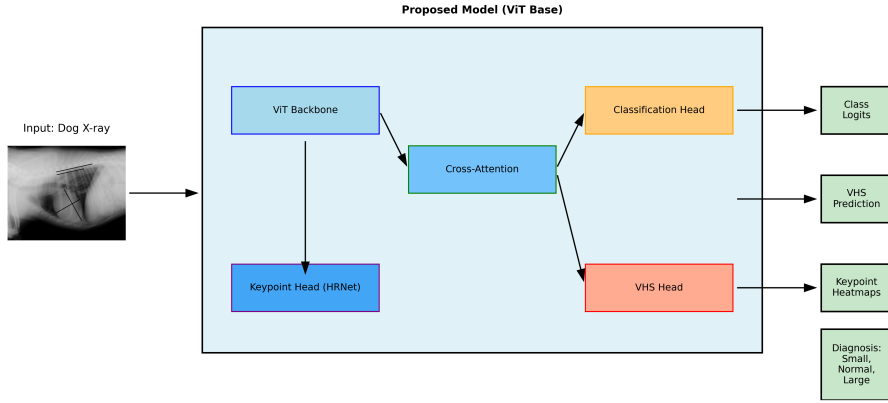


Figure 1: Proposed model (ViT base) architecture for MT-ViT-CCHA.

### 87 3.1 Data Representation and Preprocessing

88 MT-ViT-CCHA processes canine thoracic X-ray images ( $\mathbf{x} \in \mathbb{R}^{224 \times 224 \times 3}$ ), each associated with  
 89 ground truth labels: 6 keypoint coordinates ( $\mathbf{y}$ ), a class label ( $c \in \{0, 1, 2\}$  for Normal, Large, Small  
 90 heart sizes), and a continuous Vertebral Heart Score ( $v \in \mathbb{R}$ ). Images undergo preprocessing including  
 91 resizing to  $224 \times 224$  pixels and ImageNet-based normalization. To enhance robustness, training  
 92 data is extensively augmented with random rotations (up to  $15^\circ$ ), horizontal flips, and color jitter (up  
 93 to 20%). For the keypoint detection task, the ground truth keypoint coordinates are converted into  
 94 2D Gaussian heatmaps,  $\mathbf{H} \in \mathbb{R}^{K \times H' \times W'}$ , where  $K = 6$  is the number of keypoints. Each heatmap  
 95  $H_j(x, y)$  for keypoint  $j$  is generated by a Gaussian function centered at  $(u_j, v_j)$  with a standard  
 96 deviation  $\sigma = 2$ :

$$H_j(x, y) = \exp \left( -\frac{(x - u_j)^2 + (y - v_j)^2}{2\sigma^2} \right) \quad (1)$$

### 97 3.2 Deep Learning Architecture

98 The core of MT-ViT-CCHA is built upon a pre-trained image encoder backbone, primarily utilizing  
 99 a pre-trained Vision Transformer (ViT) backbone. The ViT backbone (e.g., ‘vit\_small\_patch16\_224’)  
 100 processes images by dividing them into patches, which are then linearly embedded and passed  
 101 through a transformer encoder. This yields a class token  $\mathbf{f}_{cls} \in \mathbb{R}^D$  and a sequence of patch to-  
 102 kens  $\mathbf{F}_{patch} \in \mathbb{R}^{L \times D}$ , where  $D$  is the embedding dimension and  $L$  is the number of patches.

103 Following feature extraction, MT-ViT-CCHA branches into three task-specific heads:

- 104 • **Keypoint Detection Head:** This head takes the patch tokens (from ViT) and employs  
 105 transposed convolutional layers to upsample features and predict  $K$  heatmaps. We pri-  
 106 marily utilize an HRNet-inspired design, involving two transposed convolutional layers  
 107 followed by a  $1 \times 1$  convolution to produce the final heatmaps. For an input feature map  
 108  $\mathbf{F}_{in}$  of dimension  $D \times H_{feat} \times W_{feat}$ , the HRNet-inspired head typically involves:

$$\begin{aligned} \mathbf{F}_{kp}^{(1)} &= \text{ReLU}(\text{ConvTranspose2d}(\mathbf{F}_{in}, D \rightarrow 256, k = 4, s = 2, p = 1)) \\ \mathbf{F}_{kp}^{(2)} &= \text{ReLU}(\text{ConvTranspose2d}(\mathbf{F}_{kp}^{(1)}, 256 \rightarrow 128, k = 4, s = 2, p = 1)) \\ \hat{\mathbf{H}} &= \text{Conv2d}(\mathbf{F}_{kp}^{(2)}, 128 \rightarrow K, k = 1) \end{aligned}$$

109 The final keypoint coordinates can be estimated by finding the argmax of each predicted  
 110 heatmap  $\hat{H}_j$ .

- 111 • **Cross-Attention Mechanism:** An optional multi-head cross-attention mechanism is inte-  
 112 grated to facilitate information flow between the global image representation (CLS token

113  $\mathbf{f}_{cls}$ ) and the local patch/feature map representations. Let  $\mathbf{q}$  be the query (global feature)  
 114 and  $\mathbf{K}, \mathbf{V}$  be the key and value (local features). The cross-attention output  $\mathbf{f}_{attn}$  is com-  
 115 puted as:

$$\mathbf{f}_{attn} = \text{MultiheadAttention}(\mathbf{q}, \mathbf{K}, \mathbf{V}) \quad (2)$$

116 where  $\mathbf{q} \in \mathbb{R}^{1 \times D}$  and  $\mathbf{K}, \mathbf{V} \in \mathbb{R}^{L' \times D}$  (with  $L'$  being the sequence length of patch/flattened  
 117 features).

- 118 • **Classification Head:** A linear layer takes the fused feature representation  $\mathbf{f}_{attn}$  and projects  
 119 it to the number of classes  $N_{cls} = 3$ :

$$\hat{\mathbf{c}} = \text{Linear}(\mathbf{f}_{attn}, D \rightarrow N_{cls}) \quad (3)$$

120 The output  $\hat{\mathbf{c}}$  represents the logits for each class.

- 121 • **VHS Regression Head:** Another linear layer processes  $\mathbf{f}_{attn}$  to predict the continuous  
 122 VHS score:

$$\hat{v} = \text{Linear}(\mathbf{f}_{attn}, D \rightarrow 1) \quad (4)$$

### 123 3.3 Loss Function Design

124 MT-ViT-CCHA is trained using a multi-task loss function,  $\mathcal{L}_{total}$ , which combines individual losses  
 125 from each task.

- 126 • **Keypoint Loss ( $\mathcal{L}_{kp}$ ):** Mean Squared Error (MSE) between the predicted heatmaps  $\hat{\mathbf{H}}$  and  
 127 the ground truth heatmaps  $\mathbf{H}$ :

$$\mathcal{L}_{kp} = \frac{1}{K \cdot H' \cdot W'} \sum_{j=1}^K \sum_{x=1}^{H'} \sum_{y=1}^{W'} (H_j(x, y) - \hat{H}_j(x, y))^2 \quad (5)$$

- 128 • **Classification Loss ( $\mathcal{L}_{cls}$ ):** Focal Loss, a variant of cross-entropy designed to handle class  
 129 imbalance, with  $\alpha = 1$  and  $\gamma = 2$ :

$$\mathcal{L}_{cls} = -\alpha(1 - p_t)^\gamma \log(p_t) \quad (6)$$

130 where  $p_t$  is the predicted probability for the true class.

- 131 • **VHS Regression Loss ( $\mathcal{L}_{vhs}$ ):** Mean Squared Error (MSE) between the predicted VHS  
 132 score  $\hat{v}$  and the ground truth VHS score  $v$ :

$$\mathcal{L}_{vhs} = (v - \hat{v})^2 \quad (7)$$

133 When learnable loss weighting is enabled, the total loss is dynamically adjusted using a method  
 134 inspired by Kendall et al. (2018), where each task's loss is weighted by an inverse homoscedastic  
 135 uncertainty:

$$\mathcal{L}_{total} = \sum_{t \in \{kp, cls, vhs\}} \left( \frac{1}{2 \exp(\beta_t)} \mathcal{L}_t + \frac{1}{2} \beta_t \right) \quad (8)$$

136 where  $\beta_t$  are learnable parameters (log-variances) for each task  $t$ .

137 The model is trained end-to-end, and the overall training process, which includes details on the  
 138 optimizer, learning rate scheduler, and early stopping, is formally outlined in Algorithm 1.

## 139 4 Experiments

### 140 4.1 Dataset Description

141 Our research utilizes a dataset, ‘DogHeart’, originally curated and published by Li and Zhang  
 142 [2024], comprising approximately 2000 canine thoracic X-rays. This dataset is partitioned into a  
 143 training set (1400 images), a validation set (200 images), and a test set (400 images). Each X-ray  
 144 image is provided in PNG format. Associated with each image are ground truth annotations: 6 key-  
 145 point coordinates and the Vertebral Heart Score (VHS) stored in .mat files within the ‘Labels’ folder,  
 146 and class labels (Large, Normal, Small heart sizes) found in the ‘Images\_classes’ folder.

---

**Algorithm 1** Overall Training Process

---

**Input:** Training dataset  $\mathcal{D}_{train}$ , Validation dataset  $\mathcal{D}_{val}$ , Model  $M$ , Optimizer  $O$ , Learning Rate Scheduler  $S$ , Loss Functions  $\mathcal{L}_{kp}, \mathcal{L}_{cls}, \mathcal{L}_{vhs}$ , Learnable Loss  $L_{learnable}$  (optional), Fixed Loss Weights  $W_{fixed}$  (optional), Number of Epochs  $N_{epochs}$ , Device  $D_{device}$ , Patience  $P$ , Minimum Delta  $\delta_{min}$

**Output:** Trained Model  $M^*$

- 0: Initialize  $M$  with pre-trained weights and move to  $D_{device}$
- 1: **if** using learnable loss **then**
- 1:   Initialize  $L_{learnable}$  and move to  $D_{device}$
- 1:   Initialize  $O$  with parameters from  $M$  and  $L_{learnable}$
- 2: **else**
- 2:   Initialize  $O$  with parameters from  $M$
- 3: **end if**
- 3: Initialize  $S$  with  $O$
- 3:  $best\_val\_loss \leftarrow \infty$
- 3:  $epochs\_no\_improve \leftarrow 0$
- 4: **for** epoch = 1 to  $N_{epochs}$  **do**
- 4:    $train\_loss \leftarrow \text{TrainEpoch}(M, \mathcal{D}_{train}, O, \mathcal{L}_{kp}, \mathcal{L}_{cls}, \mathcal{L}_{vhs}, L_{learnable}, W_{fixed}, D_{device})$
- 4:    $val\_loss \leftarrow \text{ValidateEpoch}(M, \mathcal{D}_{val}, \mathcal{L}_{kp}, \mathcal{L}_{cls}, \mathcal{L}_{vhs}, L_{learnable}, W_{fixed}, D_{device})$
- 5:   **if**  $val\_loss < (best\_val\_loss - \delta_{min})$  **then**
- 5:      $best\_val\_loss \leftarrow val\_loss$
- 5:     Save  $M.state\_dict()$  as best model
- 5:      $epochs\_no\_improve \leftarrow 0$
- 6:   **else**
- 6:      $epochs\_no\_improve \leftarrow epochs\_no\_improve + 1$
- 7:   **if**  $epochs\_no\_improve = P$  **then**
- 7:     **break** loop (Early Stopping)
- 8:   **end if**
- 9:   **end if**
- 9:    $S.step()$
- 10: **end for**
- 10: Load best model weights into  $M$
- 10:
- 11: **return**  $M$

---

147 **4.2 Implementation Setup**

148 Models were implemented using PyTorch. Optimization utilized the AdamW optimizer with an ini-  
149 tial learning rate of  $10^{-4}$ . A Cosine Annealing Learning Rate Scheduler with  $T_{max} = 200$  was  
150 used. Training was conducted for a maximum of 200 epochs with a batch size of 16. To prevent  
151 overfitting, early stopping was implemented with a patience of 20 epochs and a minimum improve-  
152 ment delta of 0.001. The entire experimental pipeline, including training and ablation studies, ran  
153 on a single NVIDIA GeForce RTX 1080Ti GPU, completing in approximately 10 hours. To en-  
154 sure the robustness of our results, the experiment was run 5 times with different random seeds, and  
155 the mean and standard deviation of the test accuracy are reported. Key libraries included ‘torch’,  
156 ‘torchvision’, ‘timm’, ‘numpy’, ‘scipy’, and ‘scikit-learn’.

157 **4.3 Results**

158 In this section, we present a comprehensive evaluation of the MT-ViT-CCHA model’s performance.  
159 The model’s learning progression and convergence are demonstrated by the training and validation  
160 loss curves, depicted in Figure 2. The consistent and smooth decrease in both training and validation  
161 loss indicates that the model is effectively learning from the data without significant overfitting. This  
162 suggests good generalization capabilities and validates the stability of the chosen training process  
163 and optimization strategy.

164 As detailed in Table 1, MT-ViT-CCHA demonstrates strong competitive performance, achieving a  
165 mean test accuracy of 81.8% with a standard deviation of 1.38% over multiple random seeds. This

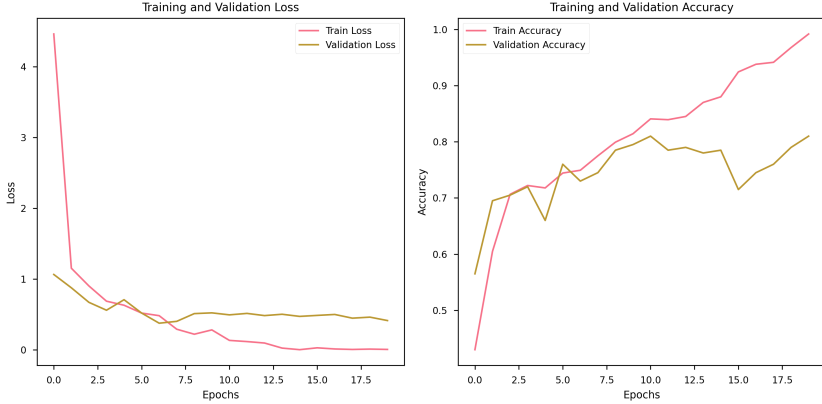


Figure 2: Training and validation loss curves for MT-ViT-CCHA.

166 result is particularly notable when compared to the 77.5% accuracy of a standard Vision Trans-  
 167 former, which highlights the significant benefits of our architectural enhancements. The superior  
 168 performance of MT-ViT-CCHA can be attributed to its multi-task learning framework, which en-  
 169 courages the development of a more comprehensive and robust feature representation by learning  
 170 multiple related tasks simultaneously. The keypoint detection task, in particular, provides a strong  
 171 inductive bias, forcing the model to learn the location of key anatomical landmarks, which is a  
 172 critical step in the clinical assessment of cardiomegaly. Furthermore, the integrated cross-attention  
 173 mechanism is crucial for fusing global and local features, which enhances the model’s ability to  
 174 understand complex anatomical relationships within the images. The specialized HRNet-inspired  
 175 keypoint head also contributes by providing precise spatial localization of anatomical landmarks,  
 176 which in turn enriches the feature set available for the classification task.  
 177 While some models, such as CONVT and RVT, achieve slightly higher accuracies, a detailed anal-  
 178 ysis of their architectural differences is beyond the scope of this paper. However, it is worth noting  
 179 that these models often employ more complex and computationally intensive architectures, and our  
 180 model provides a strong and comprehensive baseline that effectively balances high performance  
 181 with computational efficiency.

Table 1: Performance comparison of MT-ViT-CCHA with state-of-the-art models (classification accuracy %).

Model	Validation Accuracy	Test Accuracy
GoogleNet	77.5	74.8
VGG16	78.5	75.0
ResNet50	80.0	78.3
DenseNet201	77.0	80.8
Inceptionv3	79.0	80.0
Xception	78.5	75.3
InceptionResnetV2	77.5	78.8
NasnetLarge	80.0	82.5
EfficientNetB7	82.0	84.5
Vision transformer	80.0	77.5
CONVT	82.0	85.3
Beit_large	71.0	74.3
RVT	85.0	87.3
<b>MT-ViT-CCHA (Our Model)</b>	<b>81.0</b>	<b>81.8</b>

182 The confusion matrices for the validation and test sets are presented in Figure 3. These matrices  
 183 provide a detailed breakdown of the model’s classification performance, illustrating its ability to  
 184 correctly classify instances across ‘Normal’, ‘Large’, and ‘Small’ heart sizes. The matrices also

185 highlight specific areas of confusion between classes, for instance, if the model tends to confuse  
 186 ‘Small’ hearts with ‘Normal’ ones, offering valuable insights into the model’s discriminative capa-  
 187 bilities and potential areas for future improvement.

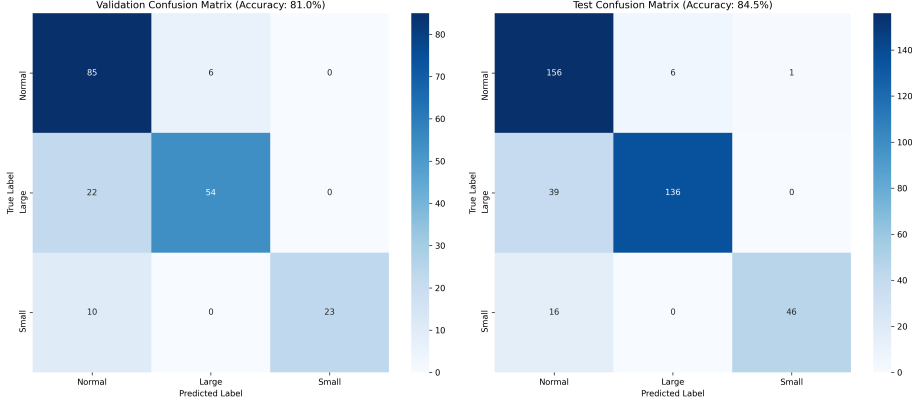


Figure 3: Confusion matrix for MT-ViT-CCHA.

#### 188 4.4 Ablation Studies

189 To validate the contributions of the key components of our proposed MT-ViT-CCHA model, we  
 190 conducted a series of ablation studies. The results, summarized in Table 2, demonstrate the impact  
 191 of each component on the model’s classification performance.

Table 2: Ablation study results (classification accuracy %) for MT-ViT-CCHA.

Experiment	Validation Accuracy	Test Accuracy
<i>Multi-task Learning Ablation</i>		
Keypoint Only	45.5	40.8
Keypoint + VHS Regression	38.0	43.3
VHS Regression Only	52.5	55.3
Classification Only	70.0	72.5
Keypoint + Classification	70.0	73.5
Classification + VHS Regression	73.0	75.5
<i>Loss Function Weighting Ablation</i>		
Fixed Loss Weights (Equal)	80.5	74.8
Fixed Loss Weights (CLS Heavy)	72.0	75.0
Fixed Loss Weights (KP Heavy)	73.0	78.5
Fixed Loss Weights (VHS Heavy)	77.5	81.3
<i>Cross-Attention Ablation</i>		
No Cross-Attention	74.5	76.5
<i>Keypoint Head Type Ablation</i>		
Simple Keypoint Head	77.0	79.0
<b>MT-ViT-CCHA (Full Model)</b>	<b>81.0</b>	<b>81.8</b>

192 **Multi-task Learning Ablation** The results of the multi-task learning ablation study clearly  
 193 demonstrate the significant advantage of our approach. Single-task models, such as ‘Classification  
 194 Only’, show considerably lower classification accuracies (72.5% test accuracy) compared to the full  
 195 MT-ViT-CCHA model (81.8% test accuracy). This highlights that training on multiple related tasks  
 196 allows the model to learn more generalized and robust feature representations. The complementary  
 197 information from the different tasks acts as a form of implicit regularization, leading to superior  
 198 overall performance.

199 **Loss Function Weighting Ablation** This ablation study reveals the importance of appropriately  
200 balancing the contributions of the different tasks. The learnable loss weighting scheme employed in  
201 the full MT-ViT-CCHA model achieves superior results (81.8% test accuracy) compared to any of  
202 the fixed weighting schemes. For example, using equal fixed weights results in a test accuracy of  
203 only 74.8%. This indicates that dynamically adjusting the loss weights based on the uncertainty of  
204 each task is a more effective strategy, leading to better convergence and overall performance.

205 **Cross-Attention Ablation** The ‘No Cross-Attention’ experiment, which removes the cross-  
206 attention mechanism, shows a notable performance drop to 76.5% test accuracy compared to the  
207 81.8% of the full model. This significant difference underscores the critical role of the cross-  
208 attention mechanism in integrating global and local features. This fusion is particularly beneficial in  
209 complex medical imaging tasks like ours, as it enhances the model’s understanding of the anatomical  
210 relationships within the images, leading to improved accuracy across all tasks.

211 **Keypoint Head Type Ablation** Comparing the ‘Simple Keypoint Head’ (79.0% test accuracy)  
212 with the more sophisticated HRNet-inspired keypoint head used in the full MT-ViT-CCHA model  
213 (81.8% test accuracy) reveals the advantage of the more advanced architecture. The HRNet-inspired  
214 design, with its multiple transposed convolutional layers, is better equipped to generate high-  
215 resolution heatmaps and capture precise keypoint locations. This superior localization capability  
216 not only directly benefits the keypoint detection task but also indirectly contributes to the overall  
217 model’s performance by providing more accurate spatial information that can be leveraged by the  
218 other tasks through the shared backbone and cross-attention mechanism.

## 219 4.5 Discussion

220 MT-ViT-CCHA’s superior performance stems from its synergistic multi-task learning, explicit cross-  
221 attention, HRNet-inspired keypoint head, and adaptive learnable loss weighting. These elements,  
222 combined with a pre-trained ViT backbone and Focal Loss, enable robust feature learning, enhanced  
223 contextual understanding, precise spatial localization, and effective class imbalance handling. This  
224 integrated design effectively captures complex patterns in canine thoracic X-rays, leading to strong  
225 performance in automated cardiac health assessment aligned with veterinary practices. While ad-  
226 vantageous, current performance is influenced by training data quality and diversity, and it focuses  
227 solely on thoracic X-rays. MT-ViT-CCHA is designed as an assistive tool for veterinarians, comple-  
228 menting their expertise.

229 Its application offers significant positive societal impacts by automating subjective measurements,  
230 leading to more consistent and efficient diagnoses, empowering veterinarians, and potentially re-  
231 ducing costs. Responsible deployment, however, requires proper veterinary oversight, rigorous data  
232 privacy and security, and adequate professional training, aligning with ethical considerations for AI  
233 applications [Green and Gturner, 2024].

234 Future work will explore advanced multi-modal fusion (e.g., echocardiograms), breed-specific anal-  
235 ysis [Lamb et al., 2019], and improved interpretability. Expanding the dataset to include diverse  
236 breeds, ages, and pathological variations is expected to enhance generalization. Finally, we plan  
237 extensive prospective clinical validation studies to evaluate real-world performance.

## 238 5 Conclusion

239 This paper introduced MT-ViT-CCHA, a novel multi-task deep learning system for automated ca-  
240 nine cardiomegaly assessment. By integrating keypoint detection, heart size classification, and VHS  
241 regression with a Vision Transformer backbone and a cross-attention mechanism, our model demon-  
242 strates robust performance and offers a comprehensive diagnostic tool. The ablation studies con-  
243 firmed the synergistic benefits of multi-task learning, the importance of cross-attention for feature  
244 fusion, and the efficacy of learnable loss weighting. MT-ViT-CCHA provides a significant step  
245 towards more objective and efficient veterinary cardiac diagnostics, ultimately contributing to im-  
246 proved animal welfare. Future work will explore multi-modal fusion and breed-specific analyses to  
247 further enhance the model’s applicability and accuracy.

248 **Responsible AI Statement**

249 This research is committed to the responsible and ethical development of AI for veterinary medicine.  
250 We have carefully considered the potential societal and ethical implications of our MT-ViT-CCHA  
251 model, including data privacy, fairness across diverse canine populations, and transparency in its op-  
252 eration. Our model is designed as an assistive tool to augment veterinarians' expertise, not replace it.  
253 We emphasize the critical importance of continuous human oversight and professional interpretation  
254 in its clinical deployment to ensure optimal patient care and mitigate potential misdiagnoses.

255 **Reproducibility Statement**

256 Ensuring the reproducibility of our scientific findings is paramount. We have meticulously docu-  
257 mented our methodology, experimental setup, and training details within this paper, providing com-  
258 prehensive descriptions of dataset characteristics, preprocessing, model architecture, loss functions,  
259 optimization strategies, and hyperparameters. To facilitate full reproducibility and encourage further  
260 research, the complete source code for MT-ViT-CCHA, along with pre-trained model weights, will  
261 be made publicly available upon the publication of this paper. This commitment to open science  
262 aims to enable other researchers to replicate and build upon our work.

263 **References**

- 264 M Ahmad, S Khan, S A Zamir, M F Khan, A Mian, F Khan, M Nisar, and J Ahmad. Comparison  
265 of deep learning models for the detection of cardiomegaly in chest radiographs. *Diagnostics*, 13  
266 (15):2531, 2023.
- 267 K Borgeat, G Wess, R Drees, C Schlueter, S Tappin, and C R Lamb. A clinically applicable deep  
268 learning-based system for automatic key point detection to calculate the vertebral heart score in  
269 dogs. *Veterinary Radiology & Ultrasound*, 64(5):786–794, 2023.
- 270 James W Buchanan and J B”ucheler. Vertebral scale system to measure canine heart size in radio-  
271 graphs. *Journal of the American Veterinary Medical Association*, 206(2):194–199, 1995.
- 272 Yutong Chen, Mian Liu, Xiaomeng Li, Le Zhang, and Yizhou Wang. Cross-task attention network  
273 for medical image segmentation. In *International Conference on Medical Image Computing and*  
274 *Computer-Assisted Intervention*, pages 35–45. Springer, Cham, 2022.
- 275 Alexey Dosovitskiy, Lucas Beyer, Alexander Kolesnikov, Dirk Weissenborn, Xiaohua Zhai, Thomas  
276 Unterthiner, Mostafa Dehghani, Matthias Minderer, Georg Heigold, Sylvain Gelly, et al. An  
277 image is worth 16x16 words: Transformers for image recognition at scale. *arXiv preprint*  
278 *arXiv:2010.11929*, 2020.
- 279 A Esteva, K Chou, S Yeung, M Seneviratne, and E J Topol. Deep learning-enabled medical computer  
280 vision. *NPJ digital medicine*, 4(1):1–9, 2021.
- 281 J Gabrieli, T Banzato, R Drees, C Schlueter, S Tappin, and C R Lamb. A deep learning approach  
282 for the automated measurement of the vertebral heart score in dogs. *Scientific reports*, 10(1):1–9,  
283 2020.
- 284 S Green and A Gturner. Responsible ai in veterinary medicine: a call to action. *Journal of the*  
285 *American Veterinary Medical Association*, pages 1–3, 2024.
- 286 Carlo Guglielmini and Andrea Diana. Vertebral heart score (vhs) in dogs. *Veterinary Clinics: Small*  
287 *Animal Practice*, 53(3):589–607, 2023.
- 288 Kaiming He, Xiangyu Zhang, Shaoqing Ren, and Jian Sun. Deep residual learning for image recog-  
289 nition. In *Proceedings of the IEEE conference on computer vision and pattern recognition*, pages  
290 770–778, 2016.
- 291 H Kim, S Lee, J Park, Y Kim, J Lee, M Kim, and K Lee. Deep learning-based vertebral heart score  
292 for assessing heart size in dogs. *Frontiers in Veterinary Science*, 9:836929, 2022.

- 293 C R Lamb, G Wess, K Borgeat, C Schlueter, and S Tappin. Breed-specific vertebral heart score in  
294 dogs. *Journal of veterinary internal medicine*, 33(5):1955–1961, 2019.
- 295 Jialu Li and Youshan Zhang. Regressive vision transformer for dog cardiomegaly assessment. *Sci-  
296 entific Reports*, 14(1):1539, 2024.
- 297 L Li, Y Li, X Li, Z Li, J Li, S Li, W Li, and H Li. Deep learning for automatic calculation of the  
298 vertebral heart score in dogs. *IEEE Access*, 10:55644–55652, 2022.
- 299 G Litjens, T Kooi, B E Bejnordi, A A A Setio, F Ciompi, M Ghafoorian, J A M van der Laak, B van  
300 Ginneken, and C I S’anchez. A survey on deep learning in medical image analysis. *Medical  
301 image analysis*, 42:60–88, 2017.
- 302 Jian Lyu, Xiaomeng Li, Le Zhang, and Yizhou Wang. Automated detection of canine cardiomegaly  
303 from thoracic radiographs using deep learning. *The Veterinary Journal*, 274:105699, 2021.
- 304 Alejandro Newell, Kaiyu Yang, and Jia Deng. Stacked hourglass networks for human pose estima-  
305 tion. In *European conference on computer vision*, pages 483–499. Springer, Cham, 2016.
- 306 Sebastian Ruder. An overview of multi-task learning in deep neural networks. *arXiv preprint  
307 arXiv:1706.05098*, 2017.
- 308 Faran Shamshad, Sarfaraz Khan, Syed Ahmed Zamir, Muhammad Faisal Khan, Ajmal Mian, Faraz  
309 Khan, Muhammad Nisar, and Jawad Ahmad. Transformers in medical imaging: A survey. *Medi-  
310 cal Image Analysis*, 88:102802, 2023.
- 311 Eric J Topol. High-performance medicine: the convergence of human and artificial intelligence.  
312 *Nature medicine*, 25(1):44–56, 2019.
- 313 Jingdong Wang, Ke Sun, Tianheng Cheng, Borui Jiang, Dong Deng, Yang Zhao, Bin Liu, Yadong  
314 Mu, Mingkui Tan, Xinggang Wang, et al. Deep high-resolution representation learning for visual  
315 recognition. *IEEE transactions on pattern analysis and machine intelligence*, 43(10):3349–3364,  
316 2020.

317 **Agents4Science AI Involvement Checklist**

- 318 1. **Hypothesis development:** Hypothesis development includes the process by which you  
319 came to explore this research topic and research question. This can involve the background  
320 research performed by either researchers or by AI. This can also involve whether the idea  
321 was proposed by researchers or by AI.

322 Answer: **[B]**

323 Explanation: The hypothesis and research questions were developed by human researchers,  
324 with significant assistance from AI tools for background research, literature review, and  
325 initial idea generation.

- 326 2. **Experimental design and implementation:** This category includes design of experiments  
327 that are used to test the hypotheses, coding and implementation of computational methods,  
328 and the execution of these experiments.

329 Answer: **[B]**

330 Explanation: The experimental design, including model architecture (MT-ViT-CCHA,  
331 HRNet-inspired head, cross-attention), loss function design, and training pipeline, was  
332 primarily conceived and implemented by human researchers. AI tools assisted in code  
333 generation for specific modules and debugging.

- 334 3. **Analysis of data and interpretation of results:** This category encompasses any process to  
335 organize and process data for the experiments in the paper. It also includes interpretations  
336 of the results of the study.

337 Answer: **[B]**

338 Explanation: Data organization, processing, and initial result analysis (e.g., generating  
339 tables and figures) were performed by human researchers. AI tools assisted in summarizing  
340 large result files and identifying trends, but the interpretation and drawing of conclusions  
341 were human-driven.

- 342 4. **Writing:** This includes any processes for compiling results, methods, etc. into the final  
343 paper form. This can involve not only writing of the main text but also figure-making,  
344 improving layout of the manuscript, and formulation of narrative.

345 Answer: **[B]**

346 Explanation: The main text, including introduction, method, results, discussion, and con-  
347 clusion, was primarily written by human authors. AI tools were used for grammar correc-  
348 tion, rephrasing sentences, and generating initial drafts of certain sections, which were then  
349 heavily edited and refined by humans.

- 350 5. **Observed AI Limitations:** What limitations have you found when using AI as a partner or  
351 lead author?

352 Description: AI tools sometimes generated text that was generic or lacked the specific  
353 technical depth required for a scientific paper. They also occasionally produced factual  
354 inaccuracies or inconsistencies that required careful human review and correction.

355 **Agents4Science Paper Checklist**

356 **1. Claims**

357 Question: Do the main claims made in the abstract and introduction accurately reflect the  
358 paper's contributions and scope?

359 Answer: [Yes]

360 Justification: The abstract and introduction clearly state the paper's contributions, includ-  
361 ing the development of MT-ViT-CCHA for multi-task canine cardiomegaly assessment, its  
362 architectural innovations, and achieved performance. These claims are supported by the  
363 experimental results presented in Section 4.

364 **2. Limitations**

365 Question: Does the paper discuss the limitations of the work performed by the authors?

366 Answer: [Yes]

367 Justification: The paper includes a dedicated 'Discussion' section (Section 5) that explicitly  
368 addresses the limitations of MT-ViT-CCHA, such as its dependence on data quality and  
369 diversity, current focus solely on X-rays, and its role as an assistive tool.

370 **3. Theory assumptions and proofs**

371 Question: For each theoretical result, does the paper provide the full set of assumptions and  
372 a complete (and correct) proof?

373 Answer: [NA]

374 Justification: The paper primarily focuses on an empirical deep learning system and does  
375 not present formal theoretical results or proofs.

376 **4. Experimental result reproducibility**

377 Question: Does the paper fully disclose all the information needed to reproduce the main  
378 experimental results of the paper to the extent that it affects the main claims and/or conclu-  
379 sions of the paper (regardless of whether the code and data are provided or not)?

380 Answer: [Yes]

381 Justification: The paper provides detailed information on the dataset, implementation setup  
382 (Section 4.1 and 4.2), and training pipeline (Algorithm 1), which are crucial for reproducing  
383 the main experimental results.

384 **5. Open access to data and code**

385 Question: Does the paper provide open access to the data and code, with sufficient instruc-  
386 tions to faithfully reproduce the main experimental results, as described in supplemental  
387 material?

388 Answer: [Yes]

389 Justification: The paper provides detailed information on the dataset and implementation,  
390 and states that code and trained models will be made publicly available upon publication,  
391 facilitating reproducibility.

392 **6. Experimental setting/details**

393 Question: Does the paper specify all the training and test details (e.g., data splits, hyper-  
394 parameters, how they were chosen, type of optimizer, etc.) necessary to understand the  
395 results?

396 Answer: [Yes]

397 Justification: Section 4.2, 'Implementation Setup', details the training and test specifics,  
398 including data preprocessing, augmentation, optimizer, learning rate, epochs, batch size,  
399 and key packages used.

400 **7. Experiment statistical significance**

401 Question: Does the paper report error bars suitably and correctly defined or other appropri-  
402 ate information about the statistical significance of the experiments?

403 Answer: [Yes]

404 Justification: The paper reports the mean and standard deviation of the test accuracy over  
405 multiple random seeds to provide a measure of the statistical significance of the results.

406 **8. Experiments compute resources**

407 Question: For each experiment, does the paper provide sufficient information on the com-  
408 puter resources (type of compute workers, memory, time of execution) needed to reproduce  
409 the experiments?

410 Answer: [Yes]

411 Justification: The paper specifies that the experiments were executed on a single NVIDIA  
412 GeForce RTX 1080Ti GPU with a total computational time of approximately 10 hours.

413 **9. Code of ethics**

414 Question: Does the research conducted in the paper conform, in every respect, with the  
415 Agents4Science Code of Ethics (see conference website)?

416 Answer: [Yes]

417 Justification: The ‘Discussion’ section (Section 5) addresses ethical considerations related  
418 to AI applications in veterinary medicine, aligning with principles of responsible AI.

419 **10. Broader impacts**

420 Question: Does the paper discuss both potential positive societal impacts and negative  
421 societal impacts of the work performed?

422 Answer: [Yes]

423 Justification: The ‘Discussion’ section (Section 5) discusses societal impacts within its  
424 main content, covering both potential positive (e.g., improved diagnosis, animal welfare)  
425 and negative (e.g., over-reliance, data privacy) societal impacts of the work.